Overall Demonstration Experiment of STICS

Yoshiyuki FUJINO, Amane MIURA, Kazunori OKADA, Maki AKIOKA, Teruaki ORIKASA, and Hiroyuki TSUJI

In this paper, we will introduce overall demonstration experiment for STICS R&D. We combined network controller between satellite and terrestrial developed in the Term A and many equipment such as channelizer and DBF etc. which are developed in the Term B. In this overall experiment, flexible assignment capability of satellite frequency band in the case of emergency disaster compared with the normal case is shown by using large scale simulator constituted in the large anechoic chamber. As a result of this experiment, validity of the technologies developed during STICS R&D is indicated.

1 Introduction

The research and development of STICS discussed up until now was carried out specific to Term A and Term B. As a compilation of this five-year research and development, this was summarized and an overall test was planned. For this reason, this overall test is also referred to as Term C, compared to Term A and Term B.

The implementation was carried out in order to evaluate previous testing overall. This included testing equipment that was the final result of a combination of the yearly Term A satellite/terrestrial network dynamic resource control equipment function improvements and testing and as well as the various products that were developed in Term B, for example the channelizer/DBF equipment and feeding section. Tests were also carried out on the large-scale deployed reflector surface module that was used in the test of Term B. Using the above equipment, we carried out overall demonstration experiments for both Term A and Term B together.

Using this equipment, three tests were carried out: a disaster communication and reconstruction test, a terminal communication test, and a video transmission test. The simulations where carried out for normal situations and for in the event of a disaster and tests were performed with the traffic at the time of Great East Japan Earthquake as an example. Results indicated that by using the network dynamic resource control equipment based on dynamic network technology, priority calls could be connected easily for traffic concentration at the disaster site by dynamically allocating satellite resources (bandwidth) of up to six times the normal values. It also indicated that the actual channelizer/DBF band changed dynamically. With this, it also indicated that it was possible to utilize finite satellite resources effectively in the event of a disaster.

2 Implementation of overall demonstration experiment

2.1 Overall demonstration experiment positioning and overview

For the overall test in the Term A, we used the satellite/terrestrial network dynamic resource control equipment, and checked the call control operations. Along with this, we could also simulate traffic conditions at the time of the Great East Japan Earthquake from Northern Miyagi Prefecture to Southern Iwate Prefecture. First, we will briefly describe these.

The functions performed during call control operations were as described below. By implementing the following call controls for call requests from actual communication terminals, actual voice communications could be carried out by dynamically switching the route.

(1) When within a terrestrial base station area
⇒ Call requests to the terrestrial base stations
(2) When the links are not free at the terrestrial base stations or when outside the area
⇒ Call requests to the satellite stations
(3) When the links are not free at the satellite stations
⇒ If it is a general non-priority terminal, call request is lost
⇒ If it is a priority terminal, call request succeeds by disconnecting a call on a priority terminal
(4) When the terminal conducting a call via a terrestrial

base station is moved outside the area
⇒ Handover to a phone call using a satellite station

(5) Non-priority terminals and priority terminals are differentiated.

In order to clarify the usefulness and issues of the satellite/terrestrial integrated mobile communication system, we built a simulation environment by simulating a traffic environment similar to the Great East Japan Earthquake. Moreover, we checked the call control functions of actual communication terminals when a disaster occurs, and we confirmed the superiority of the priority terminals. Although its results were described in Chapter **2-7**, we will provide another overview of the simulation here.

For simulating the traffic situation of the Great East Japan Earthquake, we selected the region from Northern Miyagi Prefecture to Southern Iwate prefecture, focusing around areas with maximum seismic intensity range and surrounding coastal areas. We posited the simulation period as starting at 14:00 on 2011/03/11, before the earthquake, until 02:00 on 2011/03/12 after it struck. Moreover, for the traffic model, we used the time series data[1] of traffic at the time of the Great East Japan Earthquake, as presented by NTT DoCoMo. Figure 1 shows the simulation area and Fig. 2 shows the time series of the traffic situation. Figure 2 shows a comparison with normal conditions, for the calls outgoing from the affected areas. This shows that there was a sudden increase in traffic after the earthquake, the maximum value was recorded between 15:00 and 16:00, and then there was a gradual decrease with the passage of time.

For the simulation area, ideally the entire cover area of STICS should have been evaluated, but we restricted it to a smaller selection of areas due to computer capacity. Also, we considered the simulation period to be a period before and after the occurrence of the earthquake, and we took the point at which the traffic had reduced in the middle of the night to be the end point, being 02:00 in the morning.

From the call loss occurrence situation at the terrestrial base stations and the call loss occurrence situation at the priority terminals, we simulated and evaluated the usefulness of the satellite/terrestrial integrated mobile communication system and the priority terminal control methods. The result was, in the event of a large-scale disaster, although it was difficult for the number of links at the satellite stations assumed at this stage to accommodate the entire demand of the phone calls at the disaster site, when we paid attention especially to the priority terminals that should have established communication links, it was possible for the satellite stations to accommodate most of the calls by forcibly ending phone calls on non-priority terminals. This made the satellite stations extremely effective. Moreover, we could also confirm that in a congested state, call requests could be made with the actual communication terminal as the priority terminal, and priority controls could also be implemented, such as by establishing lines using the satellite stations.

Moreover, the outcome of Term B led to the implementation of low sidelobe technology, super multi-beam forming technology, and overall demonstration of Term B, which included implementation of the channelizer/DBF equipment and primary feeding section inside a large anechoic chamber, and further, led to a test combining the separately developed large-scale deployed reflector surface module. As part of this, we did an actual test in a state that emitted the radio waves in an anechoic chamber, and by

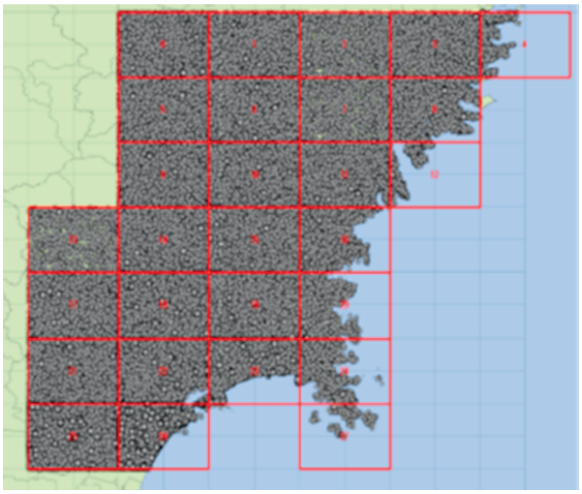

Fig. 1 Area of simulation and allocation of terminal

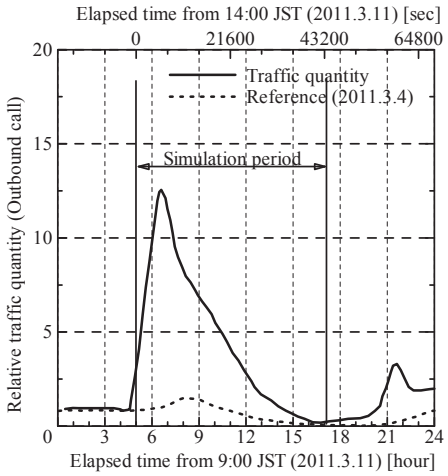

Fig. 2 Time dependence of traffic at the Earthquake[1]

confirming beam formation along with reconfiguration of the transmitting channelizer, we verified that we could switch to a desired communication bandwidth. Further, we implemented a test to confirm overall functionality and transmission characteristics through the QPSK signal for the developed channelizer/ DBF, and to transmit video and voice using the modem.

The objective of the overall Term C test was to construct products developed in Term A and B inside the anechoic chamber, and implement large-scale verification experiments using actual radio waves. For that experiment scenario, we used the scenario that was used in the overall test of Term A wherein the traffic of the disaster site increased rapidly due to earthquake. By detecting this, we increased the disaster site equivalent satellite beam bandwidth by restructuring the satellite mounted digital channelizer developed in Term B. This test is hereafter referred to as the disaster communication and reconfiguration test.

Moreover, at this time, we created equipment that simulates communication terminals and switched the functions of priority terminals and non-priority terminals, and constructed it such that the situation of non-priority terminals and communication terminals at the time of disaster could be simulated in the form of a phone call with actual voice. We thus implemented the test related to phone calls on terminals.

This test is hereafter referred to as the terminal communication test.

Further, in order to realize the extended bandwidth of the digital channelizer, we simultaneously built the ability to send and receive video. By doing this, construction was carried out such that we could detect the difference in the transmitted information when the bandwidth is either broad or narrow. This test is hereafter referred to as the video transmission test.

By carrying out the disaster communication and reconfiguration test, terminal communication test and video transmission test, respectively, which comprise the overall test, we demonstrated the effectiveness of the technology that was developed in STICS.

2.2 Composition of the test equipment

In order to implement the overall demonstration, we implemented the overall demonstration experiment with a combination of user stations, satellite stations and feederlink stations.

Figure 3 shows the test configuration of the overall demonstration experiment. The satellite/terrestrial dynamic control equipment (also referred to as the satellite/terrestrial network dynamic resource control equipment) is the test equipment for the Term A side, which generates instructions such as satellite bandwidth and DBF coefficient based on the traffic monitoring status. This equipment is intended to form part of the feederlink station from the functional standpoint, in the sense that it creates and sends commands to the satellite. The satellite station side consists of products that were developed, such as super multi-beam transmit and receiving DBF channelizer and primary feeding section, as well as a large-scale deployable antenna, wherein the instructions of commands from the feederlink station side are executed in its DBF channelizer.

Figure 4 shows the block diagram of these test systems configured inside the anechoic chamber, and Fig. 5 shows the system diagram between these devices. Moreover, Fig. 6 shows the layout of each rack. The STICS communication system is comprised of feederlink stations, satellite stations and user stations.

The functions of each station are explained below.

- Feederlink station:

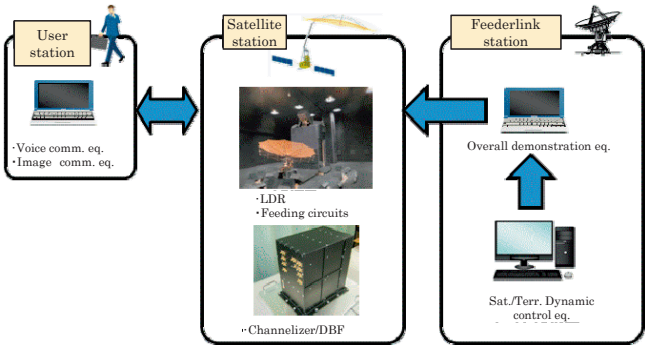

Fig. 3 Total configuration of overall demonstration

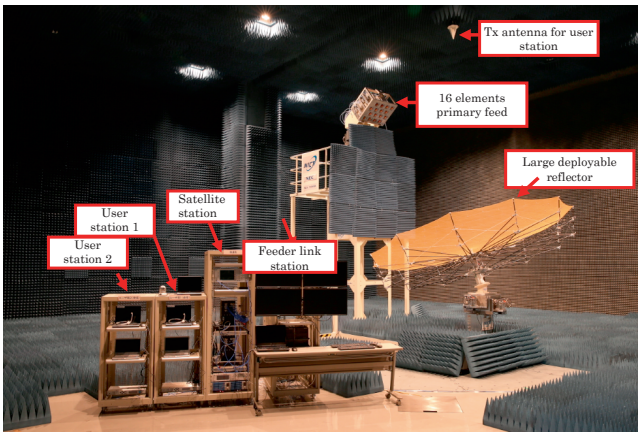

Fig. 4 Detailed configuration of testing setup

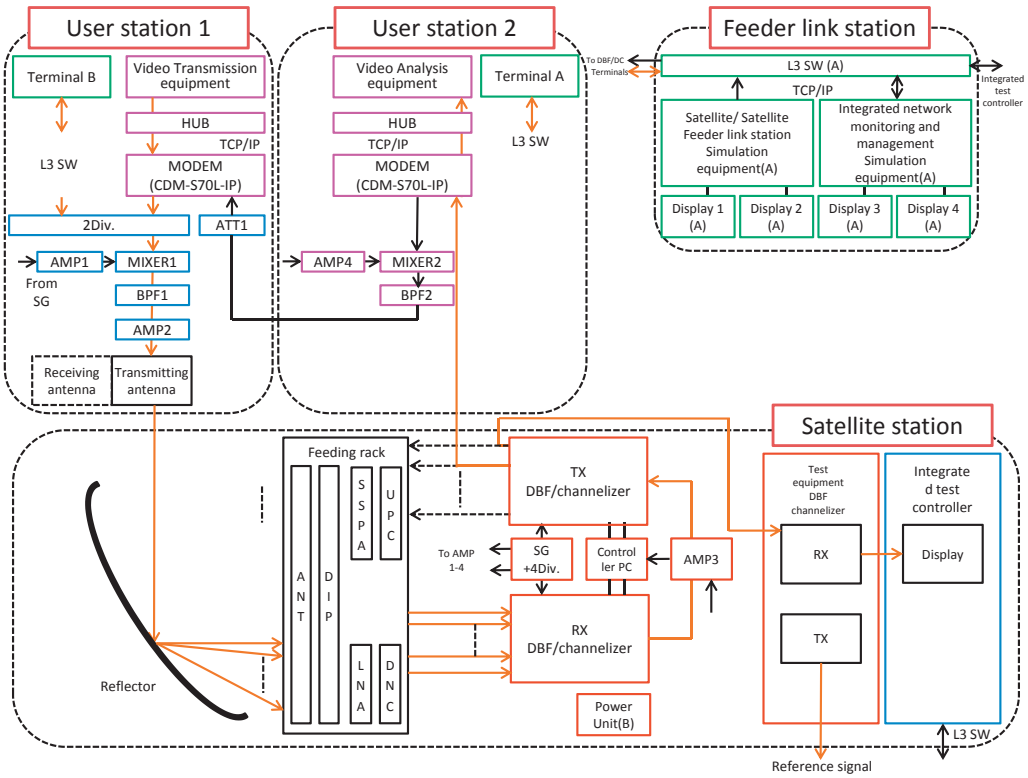

Fig. 5 Testing setup

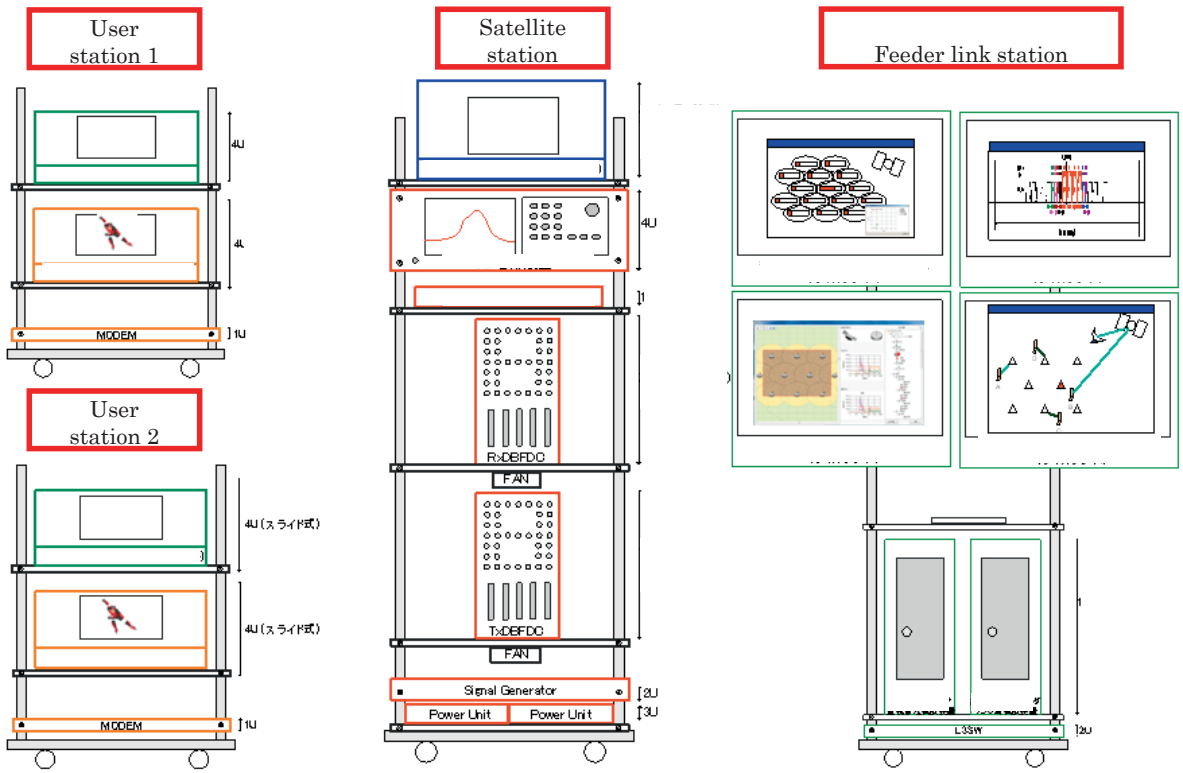

Fig. 6 Rack-mount configurations of each stations

The satellite/terrestrial dynamic control equipment that comprises the feederlink station is the equipment that serves as the functional center of STICS: it is used to sequentially understand terrestrial and satellite traffic situations and advance the test scenario. The satellite stations and the user stations operate in accordance with instructions from the feederlink station. This equipment is divided into a satellite feederlink emulator and network

dynamic resource control equipment, wherein the satellite feederlink emulator shares the satellite beam arrangement and its resource (bandwidth) allocation. The network dynamic resource control equipment is like a control tower that allocates all traffic including satellite/terrestrial, and monitors the traffic situation.

▪ Satellite station:

A satellite station has functions corresponding to the satellite in the STICS system. It consists of a large deployable antenna, small primary feeding section, transmitting channelizer/DBF equipment, and receiving channelizer/DBF equipment.

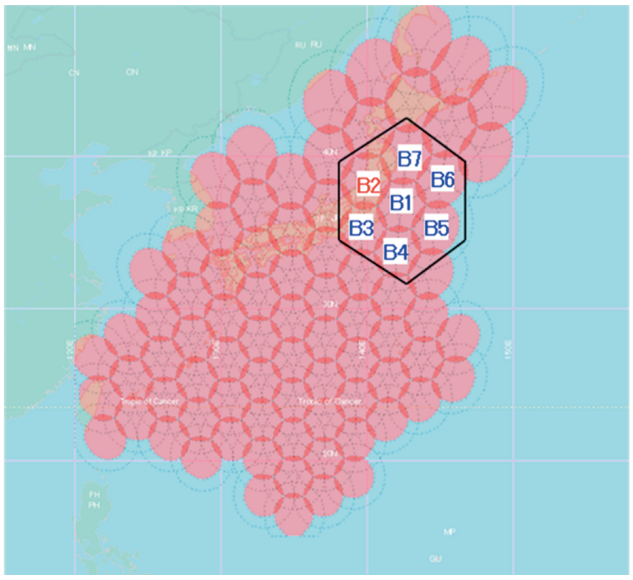

Fig. 7 Beam allocations

▪ User station:

User stations consist of voice communication equipment and video transmission and analysis equipment. The voice communication equipment is used during scenario tests, and the video transmission and analysis equipment is used during video transmission tests. Two user stations have been created that share identical functions.

Next, we explain the flow of the overall test signals, based on the test system diagram of Fig. 5. Voice signals and video signals from the user stations were sent through the user station's sending antenna, which was on the anechoic chamber ceiling. These signals were received by the satellite station.

Specifically, it is reflected by a large-scale deployable antenna of the satellite station, converted to an electric signal in the small primary feeding section, and input into the receiving channelizer DBF equipment. This equipment first uses the DBF to form the beam, then performs band conversion in the channelizer. The post conversion signal is downlinked on the feeder link side, but this function was confirmed by a hardwire connection, instead of by transmitting radio waves. Hence, the receiving signal is wrapped as it is on the feeder link side, and for that, it is input from

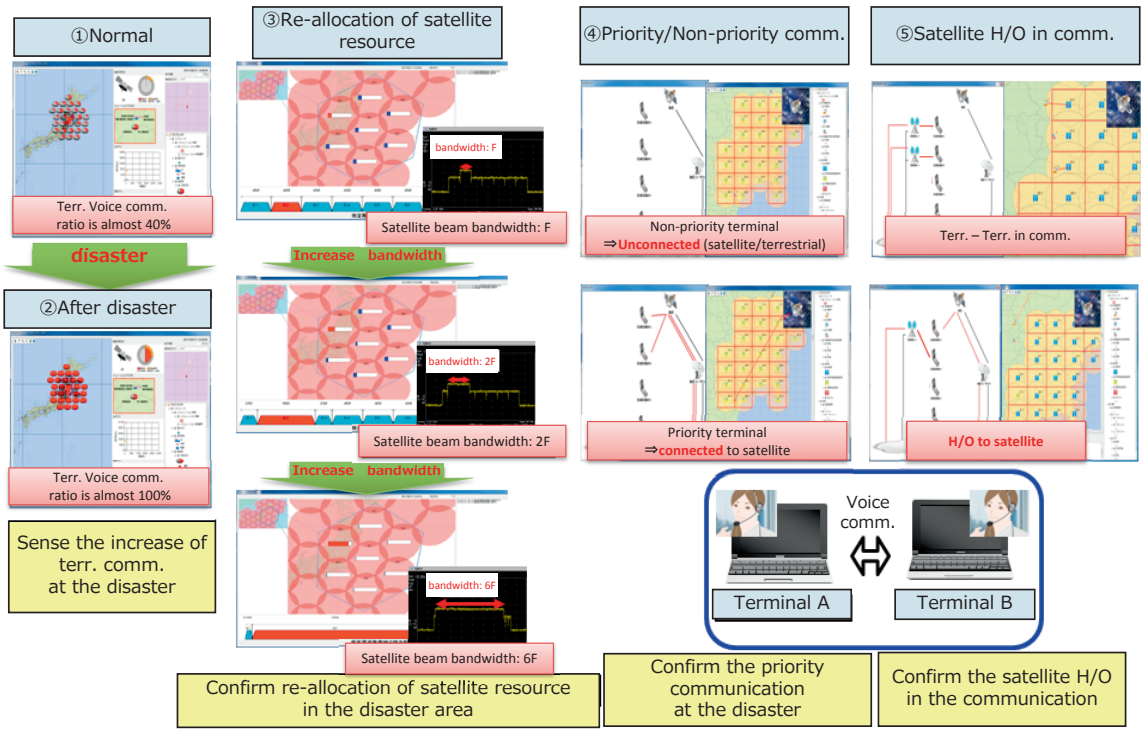

Fig. 8 Outline of overall demonstration assumed for disaster

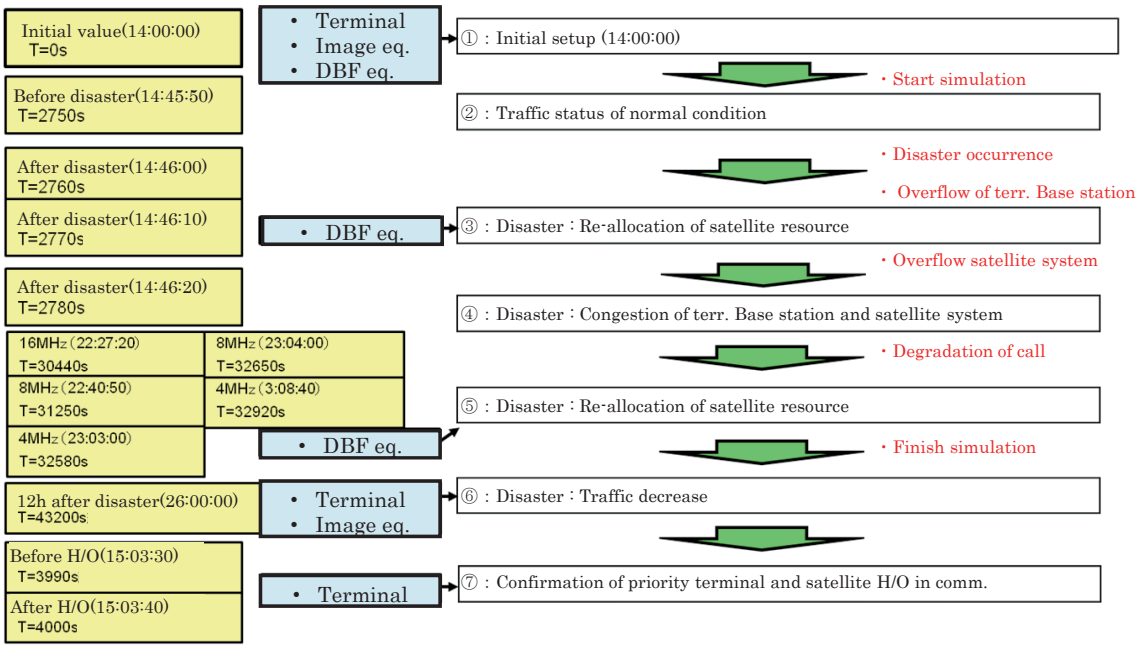

Fig. 9 Testing scenario (A series of procedure on the satellite at the disaster)

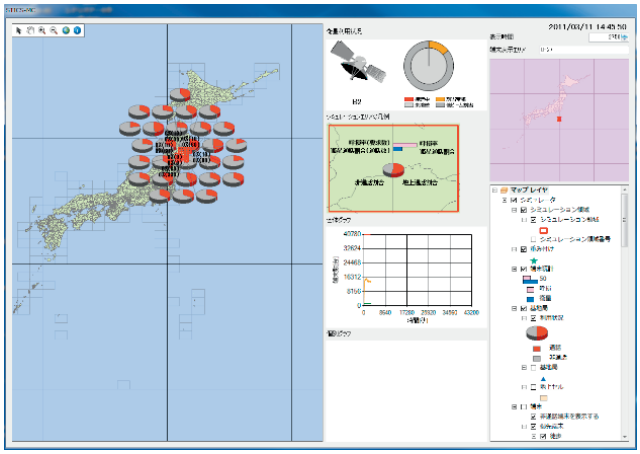

Fig. 10 Normal traffic (Network dynamic resource control equipment)

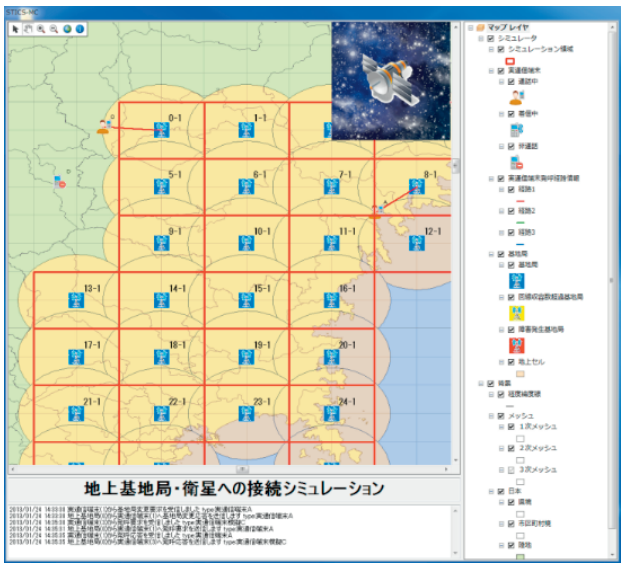

Fig. 11 Normal traffic (Network dynamic resource control equipment)

the feeder link side into the sending channelizer DBF in the satellite station. After using this equipment's channelizer to convert signals similar to that on the receiving side, it uses the DBF to form the sending beam. After that, the signal is transmitted to the user station through hardwire. This is because the sending and receiving system, using an anechoic chamber, only supports receiving.

2.3 Disaster communication reconfiguration test

2.3.1 Scope of simulation

Figure 7 shows the beam layout used in the disaster communication reconfiguration test. The disaster area was taken as the disaster site of the Great East Japan Earthquake (Miyagi Prefecture vicinity) (red circle part B2). The black hexagon shows the simulation area of the test. In the test, the satellite resources were concentrated on the disaster area during the disaster. Moreover, we input scenarios such as traffic change over time, the terrestrial non-functional base station situation, etc. into the dynamic control equipment for normal times and during a disaster, and this shows that appropriate satellite resources can be selected according to the traffic volume.

2.3.2 Disaster communication reconfiguration test

Figure 8 shows an overview of the disaster communication reconfiguration test, assuming a disaster. For the disaster and time series changes, we took the Great East Japan Earthquake as the example, and built a scenario for the disaster occurrence and the sequence of responses on the satellite side. Figure 9 shows the test scenario. Simulation start time was taken as 14:00:00 on 2011/3/11, and elapsed time is expressed as T (sec). The disaster struck at 14:46, so T=2760 (sec). Also, starting immediately after the disaster, traffic increased in the disaster area, so the integrated network monitoring and management simulation equipment that detected this gave instruction for bandwidth increase to the satellite side by using the channelizer, and on the satellite side, the corresponding beam's bandwidth was increased. Normally, the bandwidth of this beam is 4 MHz, but this was expanded to 8 and 16 MHz in steps, and it was finally expanded to 25 MHz. This situation continued until the traffic calmed down, and at T=30400 (sec) (22:27:20) it was brought back to 16 MHz, at T=32650 (sec) (23:04:00) it was brought back to 8 MHz, and returned to the normal 4 MHz at T=32920 (sec) (23:08:40).

First, Figures 10 and 11 show the traffic situation (Step 2 at normal times (T=2750 (sec)). From Figure 10, we confirmed that the ratio of phone calls to the terrestrial network capacity was about 40%. Moreover, from Figure 11, we confirmed that the state of the base stations was normal (blue color) in the entire area.

Figures 12 to 14 show the traffic situation of satellite stations at normal times. The satellite resource allocation at normal times was the resource allocation in equal intervals (4 MHz) within repeating 7-cell reuse frequencies, as understood from the lower part of Fig. 12. Moreover, the upper part of Fig. 12 shows that there is a correlation between the beam layout and satellite resource allocation, with the disaster site beams indicated specifically in red color and others in light blue color, which also indicates that allocation was done evenly for 7-cell beams. Figure 13 shows the change over time of the satellite capacity, which is also a normal situation. Figure 14 shows the DBF band related to disaster site beam at this time. This is also even allocation at 4 MHz of bandwidth.

Next, Figures 15 and 16 show the traffic situation immediately after the disaster (T=2770 (sec)) (Step 3). From Figure 15, we confirmed that the terrestrial phone call ratio is almost 100%, and from the pink bar graph, we confirmed that there were call losses at some of the base stations.

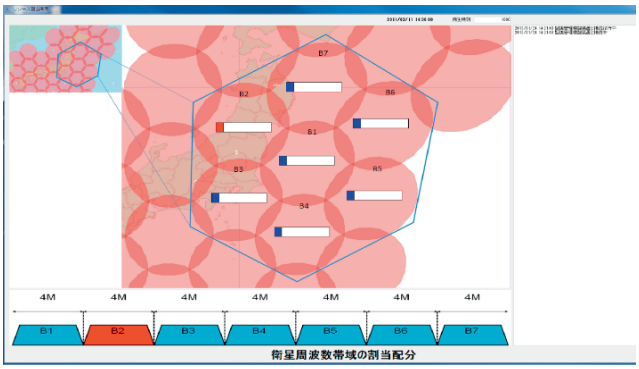

Fig. 12 Normal traffic (frequency allocation)

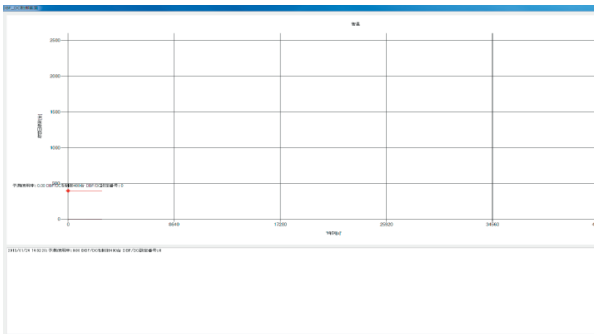

Fig. 13 Normal traffic (Satellite feederlink station emulator)

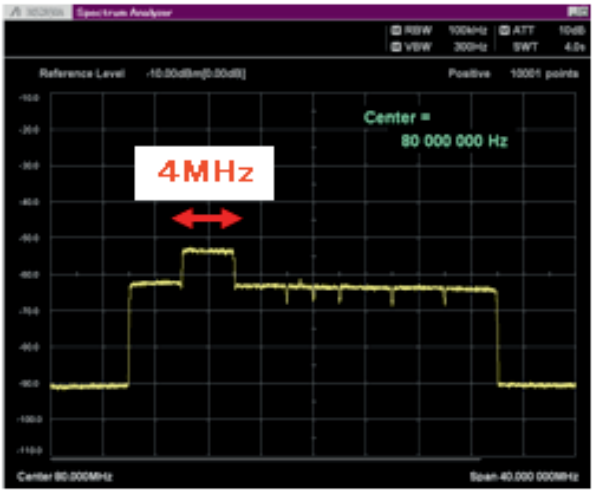

Fig. 14 Normal traffic (DBF test equipment)

Moreover, Figure 16 shows the situation of the base stations, indicating that system capacity was exceeded (yellow color). Figures 17 to 19 show the traffic situation of satellite stations at the time of the disaster. As shown in red at the lower part of Fig. 17, some of the beam band was expanded from the normal 4 to 25 MHz, and its status at the disaster site is evidenced by the beam layout diagram on the upper part of the Fig. 17. With this, each of the beams outside the disaster area had 0.5 MHz of allocation. Moreover, Figure 18 shows the change over time of disaster site beam

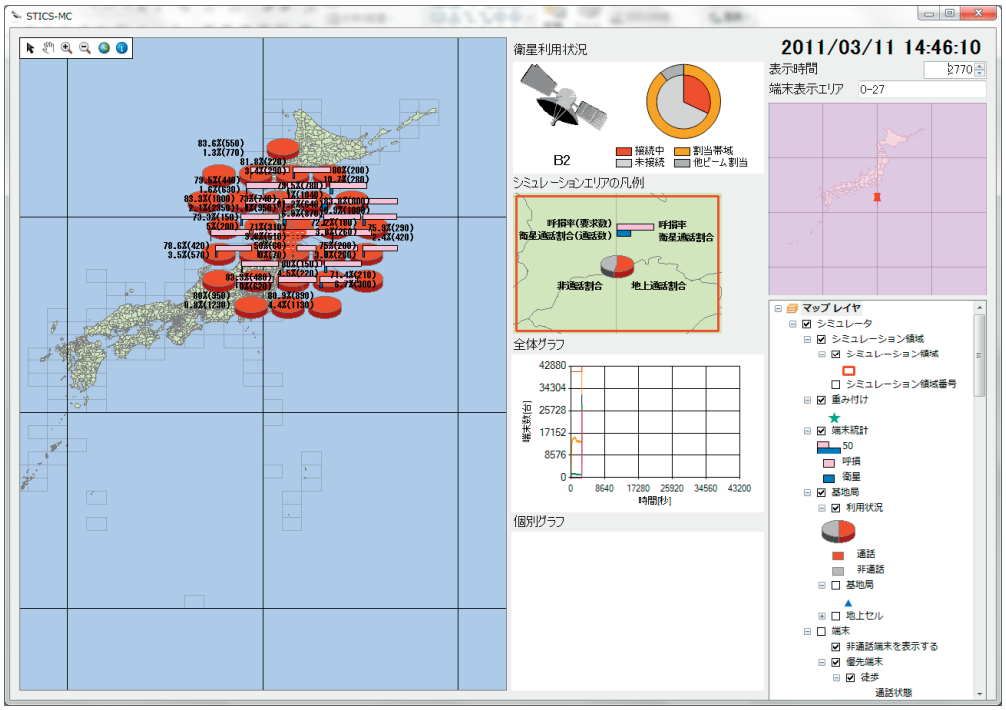

Fig. 15 Traffic state just after the disaster (Network dynamic resource control equipment)

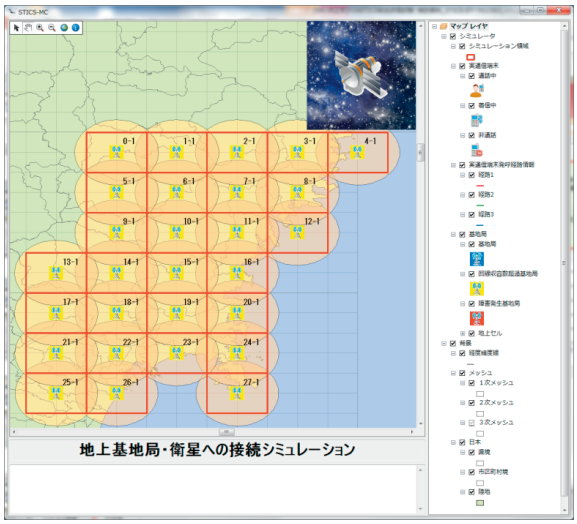

Fig. 16 Traffic state just after the disaster (Network dynamic resource control equipment)

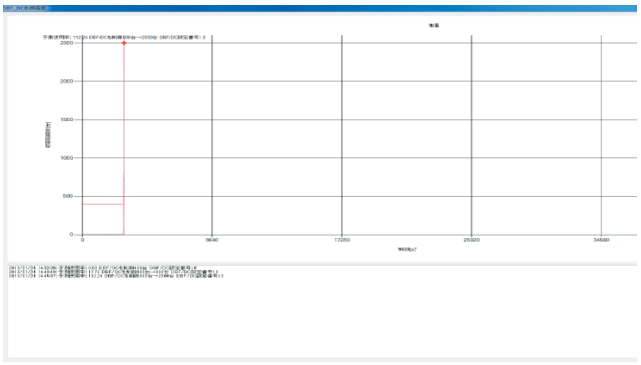

Fig. 18 Re-allocation of satellite resource (Satellite feederlink station emulator)

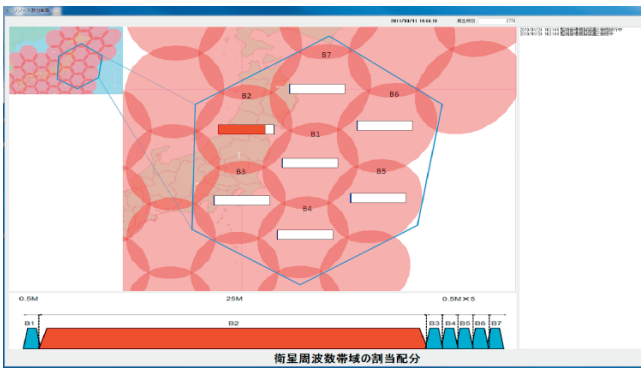

Fig. 17 Re-allocation of satellite resource (Satellite feederlink station emulator)

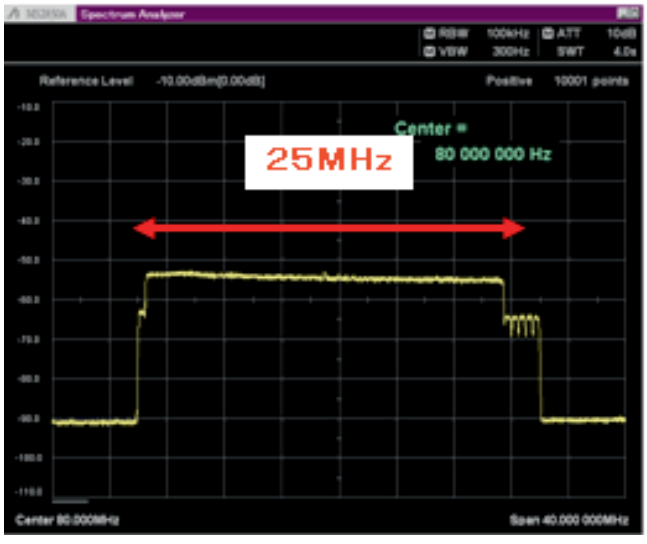

Fig. 19 Re-allocation of satellite (DBF test equipment)

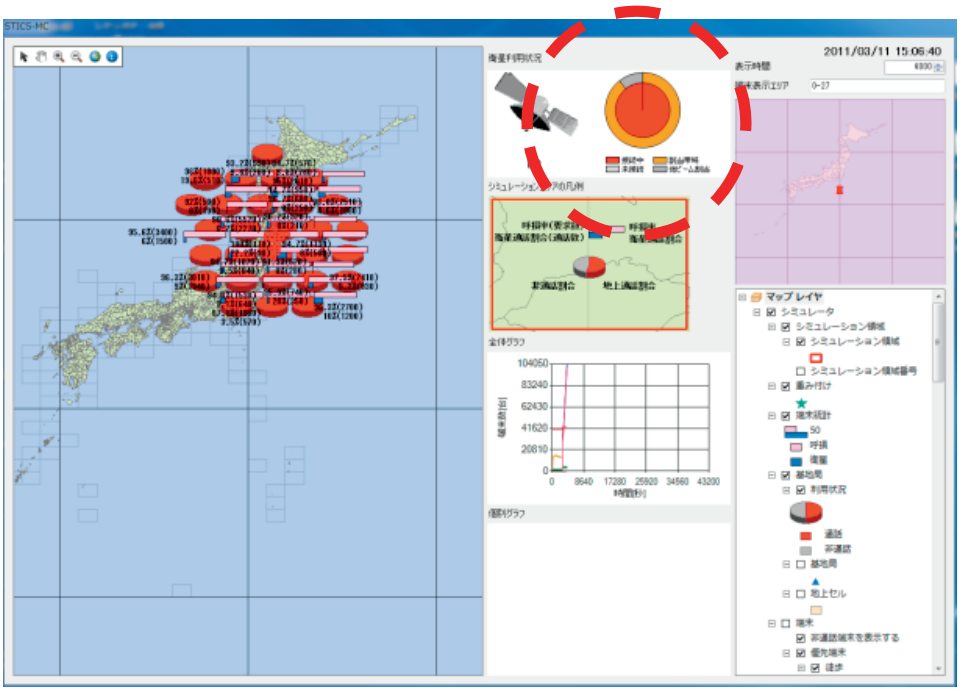

Fig. 20 Traffic congestion of terrestrial base station and satellite (Network dynamic resource control equipment)

capacity, which was raised to 6 times the normal capacity. Figure 19 shows the DBF bandwidth, and we see that this also was expanded to 25 MHz.

Figure 20 shows the congested state of terrestrial and satellite base stations at this time (Step 4). We confirmed the satellite usage situation from the pie chart (circled in red). The number of satellite connections is expressed on the inside of the pie chart, and from the fact that this is entirely in red color, we see that links were connected using the satellite's full capabilities.

Figures 21 and 22 show that after the disaster, with passage of time (T=43200 (sec)), the traffic situation calmed (Step 6). In Figure 21, the utilization ratio of terrestrial calls, shown by several pie charts on the left side, changed from red to gray color, confirming that there was surplus terrestrial call capacity. Moreover, the situation of multiple terrestrial base stations, shown in Fig. 22, was indicated by colors, whereby we confirmed that system capacity had changed from being in an excess state (yellow color) to normal (blue color).

Moreover, Figures 23 to 25 show the status of satellite resource allocation. We confirmed that the satellite resource allocation returned to the status before the disaster (normal times). Figure 23 enables us to confirm that all the beams including the disaster beam returned to the initial 4 MHz allocation.

Figure 24 shows the change over time of disaster beam links, confirming that along with a drop in traffic, it was

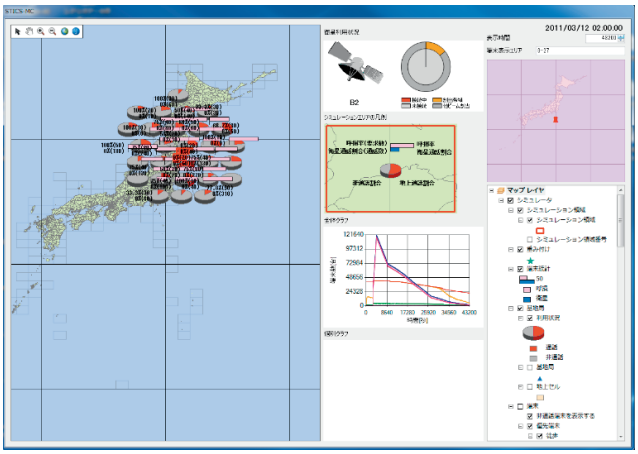

Fig. 21 Dissolved Traffic congestion (Network dynamic resource control equipment)

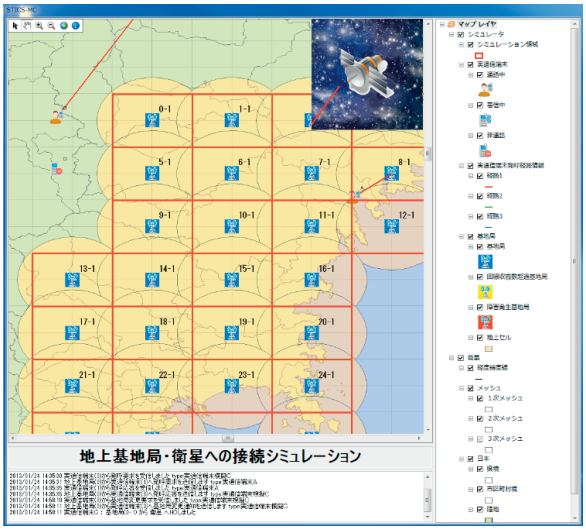

Fig. 22 Dissolved Traffic congestion (Network dynamic resource control equipment)

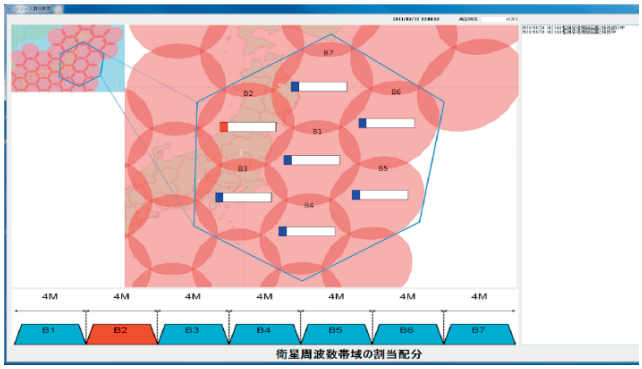

Fig. 23 Dissolved Traffic congestion (Satellite feederlink station emulator)

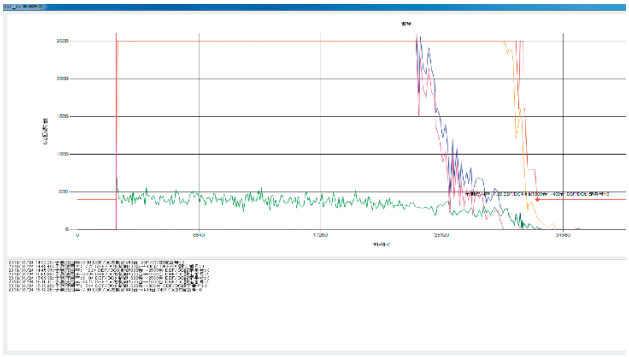

Fig. 24 Dissolved Traffic congestion (Satellite feederlink station emulator)

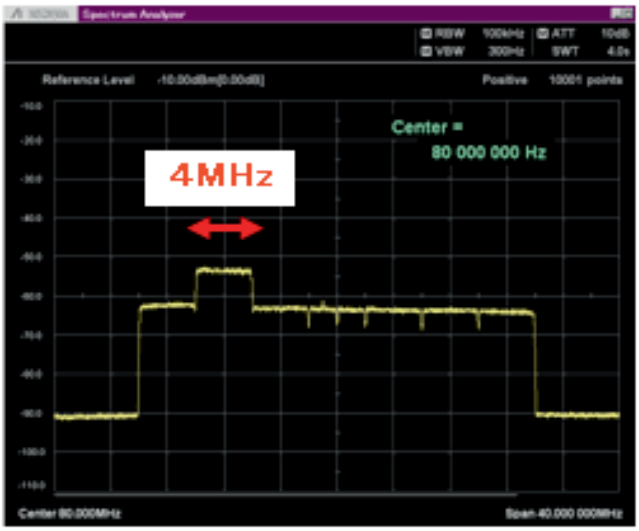

Fig. 25 Dissolved Traffic congestion (DBF test equipment)

returning to the initial number of links.

In Figure 25, we confirmed that the bandwidth of the disaster beam DBF test equipment returned to 4 MHz at that time.

2.3.3 Terminal communication test

Next, we implemented communications using actual communication terminals when communications were in an extremely congested state. Call requests were made to both non-priority terminals and priority terminals, confirming the superiority of priority terminal. Moreover, to confirm communications with continuity, which is an advantage of a satellite/terrestrial integrated mobile communication system at normal times, we confirm handover to satellite on terminals during phone calls.

After the disaster, when both terrestrial and satellite systems were extremely congested around T=4000 (sec), we checked whether phone calls were possible on an actual communication terminal (non-priority terminal). Figure 26 shows the terminal equipment view. The left side is terminal A's screen, and the right side is terminal B's screen. Now we clicked the phone call button on terminal A to try to make a call request, but it was disconnecting with status on the top left of the dialog in red color, confirming that call request was not possible on this non-priority terminal.

Next, we confirmed a phone call on an actual communication terminal (priority terminal) at the same time. Even when the base station and satellite were congested, we confirmed that a phone call is possible on the priority terminal, as seen from the view of the terminal equipment in Fig. 27. We see from Fig. 27 that after making a call request from terminal A to terminal B, communication was possible with status on the top left of the dialog changed to "In a call." Figure 28 shows the view of monitoring and management equipment, displaying the positions of terminal A and terminal B as well as the communication route. We used a headset to hear the voice of the other party, to confirm the phone call. Moreover, Figure 29 shows the phone call route of the actual communication terminal, and we see that it is via satellite.

Next, we confirmed handover to the satellite links of a terminal in a phone call at normal times.

Then, we confirmed that it was a terrestrial phone call from Figs. 30 and 31 of the network dynamic resource control equipment.

Next, we set the terminal position of the actual communication terminal A outside the area. We set the terminal outside the terrestrial area by physically moving communication terminal A outside the coverage area of the base stations, as indicated by the red circle part on the left in Fig. 32. In doing so, we could see from the red circle part on the right side of Fig. 32 that the original connection route of the actual communication terminal was via base station, and we confirmed that this was switched to via satellite.

Fig. 26 Call from user terminal (At traffic congestion: Non-priority terminal)

Fig. 27 Call from user terminal (At traffic congestion: Priority terminal)

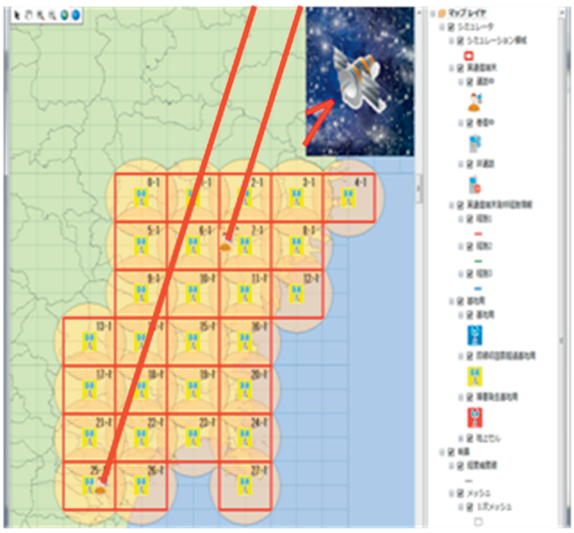

Fig. 28 Call at traffic congestion (Network dynamic resource control equipment)(Priority terminal)

Fig. 29 Call at traffic congestion (Network dynamic resource control equipment) (Priority terminal)

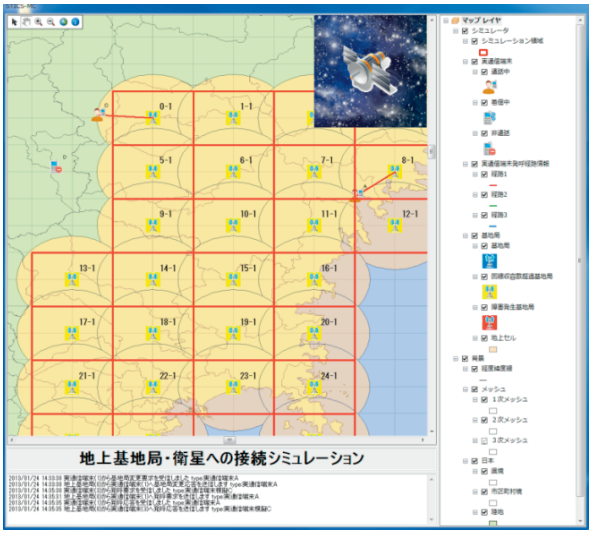

Fig. 30 Call at no traffic congestion (Network dynamic resource control equipment) (Non-priority terminal)

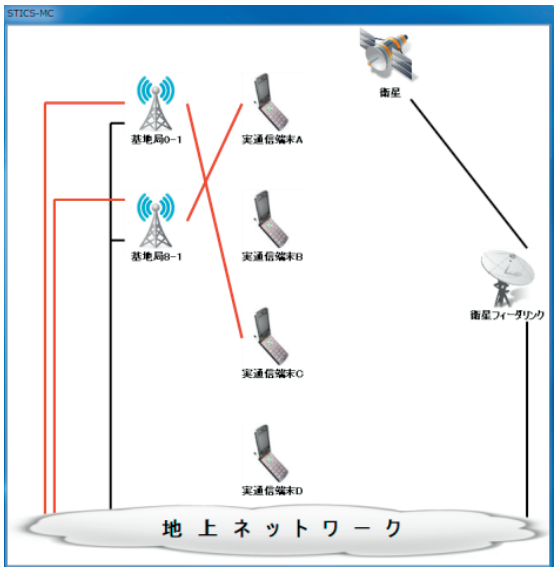

Fig. 31 Call at no traffic congestion (Network dynamic resource control equipment) (Non-priority terminal)

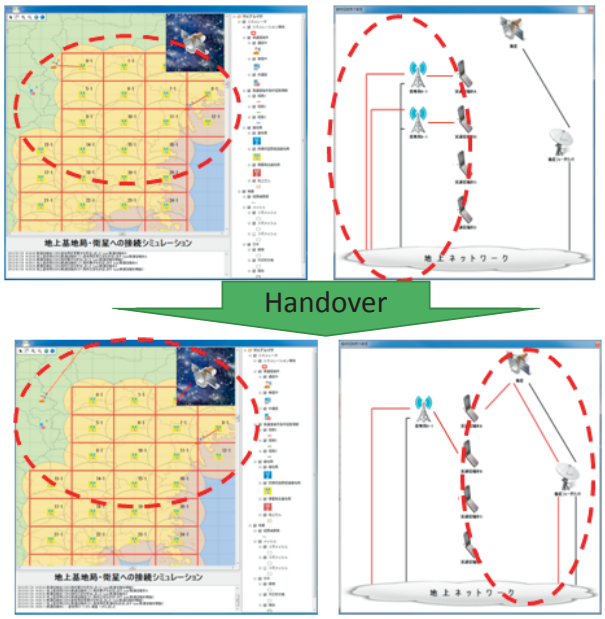

Fig. 32 Handover at no traffic congestion (Network dynamic resource control equipment) (Non-priority terminal)

2.3.4 Video transmission test

In this test, we performed the communication test using the video transmission equipment with the following test configuration. As a communication that substitutes for the equivalent of hundreds of voice communication channels, we implemented video transmission with broadband channel width, and demonstrated the efficacy of the communication system. Figure 33 shows the test configuration diagram.

Figure 33 shows the signal route of the video transmission test. The video captured by the web camera at user

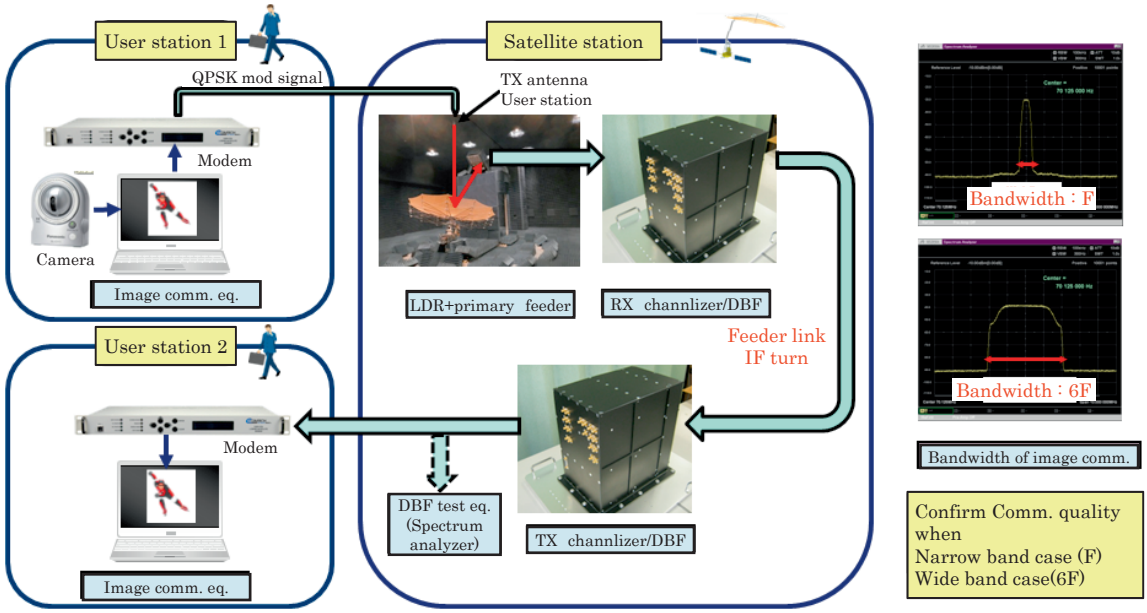

Fig. 33 Video transmission test

station 1 is input into the modem (CDM-570L-IP) through IP communication. The QPSK modulated signal in the modem is input into the receiving channelizer/DBF equipment via a large reflector and feeding rack. We took the feederlink signal output from the DBF and channelizing function part of the receiving channelizer/DBF equipment in the satellite station and returned the signal to the transmitting channelizer/DBF equipment. The RF signal output from the channelizing, DBF function part of the sending channelizer/DBF equipment was received in the modem (CDM-570-IP) of user station 2, and we confirmed the video quality in the video analysis unit (via notebook computer).

The test steps are shown here below.

Step 1: Set the overall test equipment control part to debug mode.

Step 2: Set the transmitting and receiving channelizer/DBF for the video transmission test.

Step 3: In the overall test equipment control part, set the 0.5 MHz bandwidth.

Step 4: Set the modem bandwidth to 0.5 MHz (narrow-band setting).

Step 5: Confirm spectrum in the DBF test equipment.

Step 6: Confirm video quality in the video analysis equipment.

Step 7: In the overall test equipment control part, set the 4 MHz bandwidth.

Step 8: Set the modem bandwidth to 4 MHz (broadband setting).

Step 9: Confirm spectrum in the DBF test equipment.

Step 10: Confirm video quality in the video analysis equipment.

Figure 34 shows the waveform of Step 5. Moreover, Figure 35 shows the waveform of Step 9. In the broadband spectrum, it had a trapezoidal waveform because the modem's output spectrum shape was trapezoidal.

Further, in order to facilitate confirmation of the state of bandwidth extension for channels other than the channels used, the entire signal output is set to OFF via the channelizer function. The broadband spectrum 4000 kHz setting is as per the modem constraints (about MAX 5000 kHz).

From the following waveforms, we confirmed that operations are normal for the channelizing function of the receiving channelizer/DBF equipment and transmitting channelizer/DBF equipment.

Moreover, in the tests where video transmission and analysis equipment is used, we compared the video quality in the case of a narrow-band setting and a broadband setting. As a result, we confirmed that signals dropped or delayed in narrow-band settings, and in broadband settings there were hardly any drops or delays, and we visually confirmed that smooth signal transmission could be achieved.

3 Conclusion

As a compilation of this five-year research and development of STICS, the overall demonstration experiment was

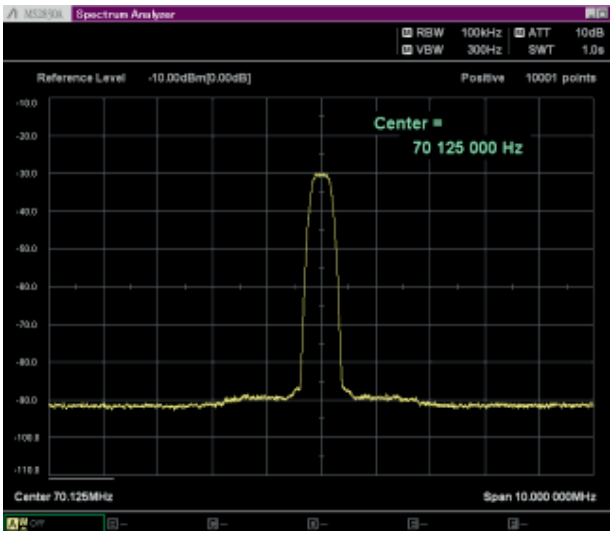

Fig. 34 Narrow band spectrum (500 kHz bandwidth)

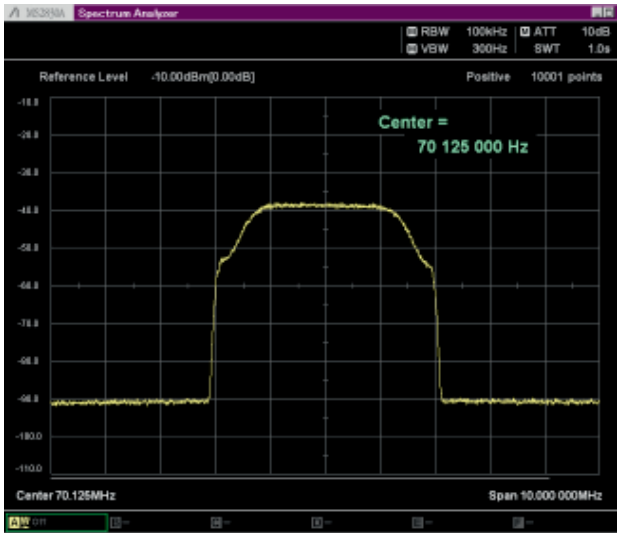

Fig. 35 Wide band spectrum (4000 kHz bandwidth)

carried out based on the outcome of the previously developed Terms A and B.

In this test, three sub-tests were performed: disaster communication reconfiguration test, terminal communication test, and video transmission test. In the disaster communication reconfiguration test, we simulated change in traffic concentration over time at the disaster site, with traffic at the time of the Great East Japan Earthquake as the base, using the network dynamic resource control equipment based on Term A's dynamic network technology. Based on this data, it was evident that satellite resources (disaster site beam bandwidth) could be allocated dynamically at up to 6 times (25 MHz) the normal (4 MHz) capacity. Moreover, in the terminal communication test, we prepared a communication terminal with non-priority call and priority call functions, and it was evident that even during a disaster, priority calls could be connected easily via satellite. Further, in the video transmission test, we used video transmission having broadband channel width, as a communication that substitutes for hundreds of voice communication channels, and we were able to make the band changing of an actual channelizer/DBF easily understood.

These tests showed that it is possible to effectively utilize finite satellite resources during disasters, and thus demonstrated the efficacy of the technology developed through STICS research and development.

4 Acknowledgments

This research was conducted under the auspices of the Ministry of Internal Affairs and Communications' "Research and Development of Satellite/Terrestrial Integrated Mobile Communications System" research contract. The authors extend thanks to all those involved.

References

1 Ministry of Internal Affairs and Communications, Meeting about communication securement in an emergency disasters, Network Infrastructure WG, Vo1.2-1 (in Japanese)

Yoshiyuki FUJINO, Dr. Eng.
Professor, Department of Electrical and Electronic Engineering, Faculty of Science and Engineering, Toyo University/Former: Senior Researcher, Space Communication Systems Laboratory, Wireless Network Research Institute (–April 2013)
Satellite Communication, Antenna, Wireless Power Transmission

Amane MIURA, Ph.D.
Senior Researcher, Space Communication Systems Laboratory, Wireless Network Research Institute
Satellite Communications, Antenna

Kazunori OKADA, Ph.D.
Senior Researcher, Space Communication Systems Laboratory, WirelessNetwork Research Institute
Mobile Communication Networks, Emergency Communications and Space Communication Systems

Maki AKIOKA, Dr. Sci.

Research Promotion Expert, Planning Office,
Wireless Network Research Institute
Solar Physics, Optical System, Space Weather

Teruaki ORIKASA, Dr. Eng.

Senior Researcher, Spacre Communication
Systems Laboratory, Wireless Network
Research Institute
Space Communication, Antenna

Hiroyuki TSUJI, Ph.D.

Senior Researcher, Space Communication
Systems Laboratory
Wireless Network Research Institute
Aircraft/Unmanned Aircraft Wireless
Communication Systems, Millimeter-wave
Broadband Mobile Communication Systems